

Comparison of Wild Type DNA Sequence of Spike Protein from SARS-CoV-2 with Optimized Sequence on The Induction of Protective Responses Against SARS-CoV-2 Challenge in Mouse Model

Sheng Jiang^{a,b}, Shuting Wu^a, Gan Zhao^c, Yue He^c, Jiawang Hou^c, Yuan Ding^c, Linlin Bao^d, Jiangning Liu^d, Chuan Qin^d, Alex Cheng^c, Brian Jiang^c, John Wu^c, Jian Yan^e, Ami Patel^f, David B. Weiner^f, Laurent Humeau^e, Kate Broderick^e, and Bin Wang^{a,b,c*}

^aKey Laboratory of Medical Molecular Virology (MOE/NHC/CAMS), School of Basic Medical Sciences, Shanghai Medical College & ^bNational Clinical Research Center for Aging and Medicine, Huashan Hospital, Fudan University, Shanghai, China.

^cAdvaccine Biopharmaceutics (Suzhou) Co. LTD, Jiangsu Province, China.

^dKey Laboratory of Human Disease Comparative Medicine, Chinese Ministry of Health, Beijing Key Laboratory for Animal Models of Emerging and Reemerging Infectious Diseases, Institute of Laboratory Animal Science, Chinese Academy of Medical Sciences and Comparative Medicine Center, Peking Union Medical College, Beijing, China.

^eInovio Pharmaceuticals, Plymouth Meeting, PA 19462, USA.

^fThe Wistar Institute, Philadelphia, PA 19104, USA.

*Corresponding Author: Bin Wang, School of Basic Medical Sciences, Fudan University, 131 Dong'an Road, 409 Fuxing Building, Shanghai, China 200032. E-mail: bwang3@fudan.edu.cn

1 **ABSTRACT**

2 COVID-19 caused by SARS-CoV-2 has been spreading worldwide. To date, several
3 vaccine candidates moved into EUA or CA applications. Although DNA vaccine is on phase
4 III clinical trial, it is a promised technology platform with many advantages. Here, we showed
5 that the pGX9501 DNA vaccine encoded the spike full-length protein-induced strong humoral
6 and cellular immune responses in mice with higher neutralizing antibodies, blocking the
7 hACE2-RBD binding against live virus infection in vitro. Importantly, higher levels of IFN- γ
8 expression in CD8+ and CD4+ T cell and specific cytotoxic lymphocyte (CTL) killings effect
9 were also observed in the pGX9501-immunized group. It provided subsequent protection
10 against virus challenges in the hACE2 transgenic mouse model. Overall, pGX9501 was a
11 promising DNA vaccine candidate against COVID-19, inducing strong humoral immunity
12 and cellular immunity that contributed to the vaccine's protective effects.

13

14 **Keywords:** SARS-CoV-2, COVID-19, Spike protein, pGX9501, DNA Vaccine, Protective
15 response

16 INTRODUCTION

17 Severe acute respiratory syndrome coronavirus 2 was a member of the *Coronaviridae* family,
18 which caused Coronavirus Disease 2019(COVID-19)^{1,2}. Over 103 million confirmed cases of
19 COVID-19, including 2 million deaths, were reported to WHO (as of February 4, 2021,
20 <https://covid19.who.int/>). SARS-CoV-2 is a single-strand positive-sense RNA virus constituted of
21 Spike protein, Nucleocapsid, Membrane protein, and Envelope protein³. The spike protein was
22 primarily associated with the infection ability of the virus and constituted of two distinct subunits,
23 namely S1 that was composed of the receptor-binding domain (RBD), and S2 consisting of the
24 transmembrane domain. The two subunits were activated after host cell cleavage and bound to
25 human angiotensin-converting enzyme 2 (hACE2) for cell entry⁴. Therefore, the spike protein
26 was an ideal immunogen candidate. The neutralization antibody which blocks RBD binding to
27 hACE2 inhibited virus infection⁵, and the mutation of amino acid of spike protein affected the
28 infectivity and stability of virus⁶.

29 Technologies to make a vaccine against the COVID-19 includes inactivated virus, subunit
30 protein, mRNA, or viral vector. DNA vaccine technology plays an essential role in vaccines.
31 Compared to other vaccine technologies, DNA vaccine is easier and cheaper to make, thermally
32 stable induces both cell-mediated and humoral immune response^{7,9}. Prior works demonstrated
33 that DNA vaccines could induce higher neutralizing antibody responses against viruses such as
34 SARS, Middle East respiratory syndrome (MERS), Zika virus¹⁰⁻¹³.

35 DNA vaccine can also induce strong T cell immunity than other vaccines. During virus
36 infection, T cell immunity plays an important role that CD4⁺ T cells are thought to provide
37 necessary secondary signals like cytokines and inflammatory signals to promote immunity, and at

38 the same time, CD8+ T cell express effector genes including Granzymes and perforin to enhance
39 its cytotoxic capacity to direct kill virus¹⁴. However, the magnitude of T cell immunity in being
40 beneficial or harmful for SARS-CoV-2 patients was unclear. Therefore, we test our DNA vaccine
41 T cell immunity and explore its role in virus infection in the hACE2-transgenic mouse model.

42 Here, we demonstrate that the pGX9501 DNA vaccine candidate, optimized codon
43 sequence for the full-length spike protein from the SARS-CoV-2, showed a significant level of
44 neutralizing antibodies and robust cellular responses and resulting in complete protection in a
45 challenge animal model.

46 **METHODS AND MATERIALS**

47 ***Animal experiment***

48 Female, C57BL/6 mice (6-8 weeks of age) and Balb/c mice (6-8 weeks of age) were
49 purchased from Beijing Vital Laboratory Animal Technology Co., Ltd. (Beijing, China) and
50 Shanghai Jiesjie Laboratory Animal Co., Ltd. (Shanghai, China), which were kept in SPF
51 condition. hACE2 transgene BALB/c mice were from the Institute of Laboratory Animal Sciences,
52 CAMS&PUMC. All animal experiments were approved by the Experimental Animals Committee
53 of SHMC.

54 The mice were injected twice via the intramuscular route (i.m.) with 25 μ g plasmid, and
55 electroporation was followed at intervals of two weeks. Serum was collected 14 days after the
56 second immunization.

57 ***Plasmid preparation***

58 Plasmids of pGX9501, pVAX1-S-WT, and pVAX1 were transformed into DH5a E. Coli,

59 respectively. A single colony was undergone expansion in a one-liter flask for culturing in LB
60 broth. Plasmids were extracted and purified by MaxPure Plasmid EF Giga Kit (Magen,
61 China). The final purified plasmids were dissolved in saline buffer at 1mg/ml. The purity was
62 measured by an agarose gel electrophoresis and a UV detector at a range of 1.8-2.0
63 OD260nm/280nm. Endotoxin in those plasmids was below 30 EU/mg by LAL test.

64 ***Rare codon analysis***

65 The sequence of wild type and the sequence optimized pGX9501 was submitted to the
66 GenScript Rare Codon Analysis Tool (<https://www.genscript.com/tools/rare-codon-analysis>).
67 From origin organism to expression host, the tool compared the difference between sequence by
68 analyzing the DNA sequence features like cis-regulatory and negative repeat elements that could
69 influence transcription and translation efficiencies after construct entered is unclear.

70 ***Antigen-specific humoral immune responses***

71 Enzyme-linked immunosorbent assay (ELISA) was used to measure the antigen-specific
72 antibody production induced by the DNA vaccinations as previously described. Briefly,
73 96-well plates were respectively coated with 0.5 μ g/ml of pre-S1 (Sino biological,
74 40591-V05H1), 0.5 μ g/ml of pre-S2 (Sino biological, 40590-V08B), and 0.17 μ g/ml of RBD
75 (Sino biological, 40592-V08B) protein (50 mM carbonate-bicarbonate buffer, pH 9.6) at 4°C
76 overnight and blocked with 5% BSA in PBST (0.05% Tween 20 in PBS) at 37°C for 1 hour.
77 The plates were incubated with diluted serum from different immunization groups for 1 hour
78 at 37°C. Antibodies were detected with HRP-conjugated goat anti-mouse IgG (Southern
79 Biotech, Birmingham, AL) after the enzymatic reaction was developed, the OD values were

80 read at 450/620 nm by an ELISA plate reader (Bio-Rad, Hercules, CA).

81 ***hACE2-RBD blocking assay***

82 The blockade of hACE2 binding to SARS-CoV-2 RBD in ELISA as previously
83 reported¹⁵. Briefly, 96-well plates were coated with 0.34 μ g/ml of RBD protein (50 mM
84 carbonate-bicarbonate buffer, pH 9.6) at 4°C overnight and blocked with 5% BSA in PBST
85 (0.05% Tween 20 in PBS) at 37°C for 1 hour. Plates were incubated with diluted serum
86 samples from different immunization groups for 1 hour at 37°C. Then, 0.12 μ g/ml of hACE2
87 (Sino Biological, 10108-H08H) was added and reacted for 1 hour at 37°C. The Goat
88 anti-Rabbit IgG-HRP (Invitrogen, 32460) and Rabbit anti-hACE2 antibody (Sino Biological,
89 10108-RP01) were used to detect the concentration of hACE2 binding with the RBD. The
90 following formula calculated the blocking ratio: Blocking Ratio= (1-(experimental
91 group/control group)) *100%.

92 ***Live virus neutralization assays***

93 Neutralization assays were performed at the Institute of Laboratory Animal Sciences,
94 CAMS&PUMC of China. Seed SARS-CoV-2 (SARS-CoV-2/WH-09/human/2020) stocks and
95 virus isolation studies were performed in Vero E6 cells, which are maintained in Dulbecco's
96 modified Eagle's medium (DMEM, Invitrogen, USA) supplemented with 10% fetal bovine
97 serum (FBS), 100 IU/mL penicillin, and 100 μ g /mL streptomycin, and incubated at 36.5 °C,
98 5% CO₂. Virus titers were determined using a standard 50% tissue culture infection dose
99 (TCID₅₀) assay. Serum samples collected from immunized animals were inactivated at 56 °C
100 for 30 min and serially diluted with a cell culture medium in two-fold steps. The diluted

101 samples were mixed with a virus suspension of 100 TCID50 in 96-well plates at a ratio of 1:1,
102 followed by 2 h incubation at 36.5 °C in a 5% CO₂ incubator. 1× 10⁴ Vero cells were then
103 added to the serum-virus mixture, and the plates were incubated for 3–5 days at 36.5 °C in a 5%
104 CO₂ incubator. Cytopathic effect (CPE) of each well was recorded under microscopes, and
105 the neutralizing titer was calculated by the dilution number of 50% protective condition.

106 ***Flow cytometry***

107 Single suspension cells from spleens and lymph nodes collected 14 days after the second
108 immunization were prepared and stimulated with 10µg/ml peptides at 37°C for 5h. Cells were
109 stained with viability dye eflour780 in PBS for 15 minutes on ice followed by washes twice
110 with PBS supplemented with 2% FBS. For the detection of cell surface antigens, cells were
111 stained with fluorochrome-tagged antibodies, as shown in the following table for 15 minutes
112 on ice. To detect intracellular cytokines or intranuclear transcription factors, cells were fixed
113 and permeabilized using an intercellular cytokine staining kit (BD) or a commercial
114 transcription factor staining kit (eBioscience). All stained samples were run on LSRII Fortessa
115 (BD) and analyzed by FlowJo (TreeStar).

Antibody	Company	Clone	Lot number
anti-Mouse CD4-APC	ebioscience	GK1.5	4329627
anti-Mouse CD8a-PerCP/Cy5.5	biolegend	53-6.7	B219152
anti-Mouse TNF α -PE	ebioscience	MP6-XT22	438513
anti-Mouse Granzyme B-PE Cyanine7	ebioscience	NGZB	4281151
anti-Mouse IFN γ -APC	ebioscience	XMG1.2	4289683

anti-Mouse IFN γ -BV421	biolegend	XMG1.2	B232596
anti-Mouse CD3e-FITC	ebioscience	145-2C11	E00061-1632
anti-Mouse IL-5-PE	ebioscience	TRFK5	12-7052-82
anti-Mouse IL-13-eFlour710	ebioscience	eBio13A	46-7133-82

116 ***SARS-CoV-2 Spike protein Peptide pool***

117 COVID-19 spike RBD peptide pool (SARS-CoV-2 Spike protein 258-518aa) published
118 previously¹⁶ was used for the study.

119 ***Cytotoxic lymphocyte (CTL) killing ability***

120 Singles suspensions of splenocytes from naïve syngeneic mice were diluted to
121 1.5×10^8 /ml by RPMI1640 with 10% FBS and 2% Penicillin and Streptomycin, respectively
122 then pulsed with or without 5ug/ml peptides as mentioned above at 37°C. After 4 hours, a
123 higher concentration of eflour450 (ebioscience, 65-0842-85) at 5mM was used to label pulsed
124 peptide cells. Cells without peptide-pulsed were labeled with a low concentration of
125 eflour450 at 0.5mM at room temperature in the dark. After being rinsed by PBS three times,
126 4×10^6 of labeled and peptides-pulsed cells and another equal number of labeled cells without
127 peptide-pulsed were adoptive transferred by tail vein injections into mice previously
128 immunized with different vaccines, respectively. Six hours later, the percentage of labeled
129 cells was detected with LSRII Fortessa flow cytometry (BD) and analyzed by FlowJo (TreeStar).
130 The following formula calculated the specific cell lysis: Specific cell lysis ability =
131 $(1 - (\text{percentage of cells incubated with peptide} / \text{percentage of cells incubated without peptide}))$
132 *100%

133 ***SARS-CoV-2 challenge Study***

134 SARS-CoV-2 (SARS-CoV-2/WH-09/human/2020/CHN) was isolated by the Institute of
135 Laboratory Animal Sciences, CAMS&PUMC. Immunized hACE2 transgenic mice were
136 infected with SARS-CoV-2 (10^6 TCID₅₀) via the nasal route in a volume of 100 μ l 7 days after
137 the final immunization. Five days after infection, the Lung was harvested for measuring virus
138 loads by qPCR and H&E staining. Before the challenge, serum was collected for ELISA to
139 evaluate the neutralizing antibody levels.

140 ***Statistical Analysis***

141 The statistical analysis methods and sample sizes (n) are specified in the results section
142 or figure legends for all quantitative data. All values are reported as means \pm sem with the
143 indicated sample size. No samples were excluded from the analysis. All relevant statistical
144 tests are two-sided. P values less than 0.05 were considered statistically significant. All
145 animal studies were performed after randomization. Statistics were performed using
146 GraphPad Prism 7 software. In all data *p<0.05, **p<0.01, ***p<0.001, and ****p<0.0001.

147 **RESULTS**

148 **Expression Level of Optimized Spike Sequence.**

149 A DNA construct, pVAX1-S-wt, made from the wild type sequence of the full-length spike
150 protein of the SARS-CoV-2 was subcloned into the pVAX1. The sequence of the same region was
151 optimized via SynCon® technology as previously described, synthesized, and cloned into pVAX1
152 as the pGX9501¹⁶. Two constructs were transfected into 293T cells in vitro parallelly under the
153 same condition and subjected into a qRT-PCR and Western blotting Analysis to compare
154 expression levels. As depicted in Figure 1A and 1B, the level of mRNA and protein expressions
155 were hundred times greater from the optimized pGX9501 over the wild type pVAX1-S-wt. We
156 further discovered that the critical differences between the two sequences were the contents of
157 negative Cis-elements, five in the wild-type, one in the optimized pGX9501 (Table 1).

158 **Effects of Antibody Production and Functional Assay**

159 To evaluate the effects of pVAX1-S-wt and pGX9501 DNA vaccines on the abilities to
160 induce specific antibodies, mice were injected twice at 25 μ g DNA vaccine each time via
161 intramuscularly (i.m) at biweekly intervals and followed by electroporation by a Cellectra2000
162 device (Figure 2A). Serum IgG samples were serial diluted and tested for binding titles against
163 recombinant spike proteins covered the receptor-binding domain (RBD), S1 region, and S2 region
164 in the extracellular domain (ECD). Levels of antibodies taken from pGX9501 immunized Balb/c,
165 or the C57/BL6 animals, were a thousand times higher than pVAX1-S-WT immunized (Figure
166 2B). In addition, these sera were also used to examine the inhibition experiment of RBD to human
167 angiotensin-converting enzyme 2 (ACE2) binding. We observed that a higher level of inhibition
168 was achieved from sera immunized with pGX9501 than pVAX1-S-WT (Figure 2C).

169 **Efficacy of protective response against SARS-CoV-2 challenge in hACE2 transgenic mice.**

170 The goal of a vaccine is to protect against disease, or ultimately against infection of the virus.

171 We examined the efficacy of protection after the DNA vaccine immunization(s) followed by a

172 challenge of SARS-CoV-2 in hACE2 transgenic animals(Figure 3A). After once or twice

173 immunizations of those transgenic mice, animals were challenged intranasally with 1×10^6

174 TCID50 of SARS-CoV-2 viruses post of 7 days from the last immunization. The virus neutralizing

175 assay was performed using serum samples from the pGX9501 immunized once or twice and the

176 samples from pVAX1 as the control. The neutralizing level from pGX9501 immunized once was

177 around 1:18 but increase significantly after the two immunizations at 1:166, compared with the

178 control (Figure 3B). The animals were sacrificed 5 days after the challenge for Analysis of viral

179 loads in lungs and pathological changes. We observed almost $6 \log_{10}$ reduction of viral loads in

180 lungs from mice immunized twice with the pGX9501, which was nearly a complete protection

181 against SARS-CoV-2 infection, whereas the 1-2 \log_{10} reductions were reached in animals

182 immunized once with pGX9501 (Figure 3C). According to the pathological Analysis H&E stained

183 lung tissue sections, the mice immunized twice was showed slight infiltration of inflammatory

184 cells in the alveolar septum and pulmonary vessels, compared with the control group (Figure

185 3D&Table 2).

186 **Effects of Cell-Mediated Immunity (CMI)**

187 DNA vaccine has a strong ability to induce CMI due to its expression in host cells and to present

188 its antigens via MHC-I and -II. To assess the CMI, mice immunized with either pGX9501 or

189 pVAX1-S-WT in Balb/c and C57/BL6 mice on day 14 after the second immunization were used to

190 isolate T cells from spleens or Lymph nodes for analyzing intracellular cytokine expressions by

191 flow cytometry. As depicted in Figure 4, percentages of IFN- γ -expressing CD4 T cells,
192 representing Th1 response, were higher in both C57/BL6 and Balb/c mice immunized with
193 pGX9501 than that of the other two groups (Figure 4A&4B). However, expressions of IL-5 and
194 IL-13 in CD4 T cells, representing Th2 response, showed no much differences among the groups
195 (Figure 4C & 4D). Levels of IFN- γ and TNF- α expressing CD8 T cells again were higher in the
196 group immunized with pGX9501 in both C57/BL6 and Balb/c mice (Figure 5A&5B). Expression
197 of Granzyme B (Gz-B) in CD8 T cells was observed as similar results as obtained as the IFN- γ
198 (Figure S1A&S1B).

199 Functional CD8 T cells serve as cytolytic killer T cells to destroy virally infected host cells,
200 resulting in a sterilizing immunity. Since its function can be tested in the in vivo CTL assay, we
201 examined the level of specific CTL killing activities in those immunized groups. We observed that
202 a significantly higher level of CTL was achieved from both Balb/c mice and C57/BL6 mice
203 immunized with pGX9501 compared with that of the other two groups (Figure 5C).

204 **DISCUSSION**

205 The COVID-19 DNA vaccine (pGX9501) has been found to induce a significantly high level
206 of immunogenicity in animal studies and human trials¹⁶. Before select candidate constructs for a
207 pre-clinical project, we found that using wild type sequence of SARS-CoV-2 Spike as a DNA
208 vaccine, pVAX-S-wt, induced poor antibody induction. To investigate the reason, we compared
209 those two head-to-heads in this study and observed that over a hundred times higher expression
210 level of mRNA had been achieved with the pGX9501 after transfected into culture cells over that
211 from the pVAX-S-wt (Figure 1A). Such a superior level was also revealed from the corresponding
212 expressed spike protein (Figure 1B). The higher expression level is translated into a higher level

213 of anti-spike antibodies, blocking RBD to hACE2 binding and neutralizing activities against live
214 viruses infecting host cells. Not only was antibody level greatly enhanced, induction of T cells,
215 including CD4 and CD8 T cells producing IFN- γ and TNF- α , were also augmented. Notably, the
216 level of cytolytic CD8 cells was significantly increased, demonstrated by the in vivo CTL assay,
217 suggesting the ability to clearance of viral infection. Finally, the codon-optimized pGX9501
218 construct effectively expresses eukaryotic cells as one of the critical factors, which could be
219 translated into higher efficiency to induce host immune responses, further providing a protective
220 response against live virus challenge with reduced lung pathogenesis in a dose-dependent manner.

221 Although optimization of codons in a foreign gene could significantly enhance its expression,
222 in general, has been reported, the over hundreds if not thousand fold increases in expression from
223 the pGX9501 to pVAX-S-wt is un-thinkable. Further rare codon analysis observed that five
224 negative Cis-regulatory elements were situated within the coding region of wild-type spike versus
225 only one with the pGX9501¹⁶ (Figure 1B). Previous studies showed that a gene expression could
226 be inhibited negative cis-regulatory elements and restored after the elements were mutated^{17,18}.
227 Thus, we reasoned that the decreasing number of negative CIS-regulatory elements in the
228 optimized pGX9501 could account for the higher mRNA and protein expression over that of wild
229 type besides the rare codon usages.

230 In SARS-CoV-2 infection, neutralizing antibodies were essential in preventing viral entry
231 and patients' prognosis. The neutralizing antibody specific to spike protein correlated with a fatal
232 outcome for patients infected with SARS-CoV-2¹⁹ and prevented viral infection during the viral
233 outbreak for normal individuals²⁰. More than 11 anti-spike monoclonal antibodies²¹ including
234 LY-CoV555²², 414-1²¹, and CB6²³ revealed high-affinity bindings to the RBD and hACE2 binding

235 inhibitions correlated to their neutralizing activities. Thus, we also evaluated the specific
236 anti-Spike binding antibody and RBD-hACE2 binding inhibition ability, in which the optimized
237 pGX9501 induced a significantly higher level of the wild type one.

238 T cell immunity was indispensable for viral clearance demonstrated in animal models
239 infected with viruses like JEV, DENV, and recent Zika²⁴⁻²⁹. In the SARS-CoV infection model,
240 enhanced CD8+ T cell resulted in earlier virus clearance and increase survival³⁰. Clinical data in
241 SARS infected patients showed that a better recovery was usually linked with T cell immunity³¹.

242 A similarity has been observed in SARS-CoV-2 infected patients in that COVID-19 patients with
243 non- to mild-symptom showed significantly higher levels of anti-SARS-CoV-2 CD4 and CD8 T
244 cells versus that of the lower level of such T cells in severe or dead patients³². Simultaneously,
245 patients infected with SARS-CoV-2 with worse disease outcomes were related to T cell
246 exhaustion³³, and lymphopenia was accentuated in symptomatic SARS-CoV-2 patients with
247 pneumonia than those without pneumonia that indicated T cell immunity was played an essential
248 protective role in pre-existing immunity against SARS-CoV-2^{32,34-36}.

249 Further supported activations of specific T cells were essential and correlated with protective
250 efficacy by the recently developed mRNA vaccines (BNT162b2 and mRNA-1273)³⁷ and
251 adenoviral vector-based one (AZD1222)³⁸. In a recent study of AD26.COV2.S Vaccine, CD8 T
252 cell immunity presents a broad spectrum of protection against SRAS-CoV-2 variants³⁹. Therefore,
253 antigen-specific T cell responses play an indispensable role against SARS-CoV-2 infectivity and
254 COVID-19 pneumonia. Therefore, T cell immunity is a crucial factor for protecting people from
255 SARS-CoV-2 infection. A DNA vaccine is known to induce higher T cell-mediated response from
256 previous studies, including the pGX9501 induced T cell responses in mice, monkeys, and humans

257 recently in phases I & II. In this study, we observed that mice immunized with the pGX9501
258 produced a higher expression level of Th1 cytokine IFN- γ and a vigorous CTL activity, which
259 indicate that both Th1 and cytotoxic T cell was involved in the immunity for protecting mice from
260 SARS-CoV-2 infection.

261 Our study found that the pGX9501 immunized twice showed a better virus clearance and
262 Lung protection than the pGX9501 immunized once. Firstly, the pGX9501 immunized twice
263 induces a higher neutralizing antibody than the group immunized once. Then, the pGX9501
264 immunized once only showed serval protection effect on virus infection, while the pGX9501
265 immunized twice protects mice from virus infection. In summary, only one dose may not induce a
266 strong enough immune response to protect the body from the virus, and the pGX9501 immunized
267 twice can. For the substantial virus clearance of the pGX9501 immunized twice group, we thought
268 that neutralizing antibody that inhibits the virus entry and cell immunity that clears the virus in the
269 body was indispensable. The neutralizing antibody the pGX9501 immunized twice induced was
270 highly correlated to the inhibition ability of virus infection¹⁹. At the same time, the mice
271 immunized twice showed a more IFN- γ and TNF- α expression of T cell, which was associated
272 with virus clearance^{26,29,34}. In conclusion, compared with the wild-type coding sequence, the
273 optimized one pGX9501 was a promising DNA candidate vaccine for preventing SARS-CoV-2,
274 and T cell immunity plays a primary role in protecting the body from SARS-CoV-2 infection.

275 **Acknowledgment**

276 This work was supported by the Chinese National Natural Science Foundation
277 (81991492 and 82041039) and National Key R&D Program of China

278 (2018YFC0840402) to B.Wang.

279 **Competing interests:** Authors declare that they have no competing interests.

FIGURES

Figure 1. Comparison of expression and antibody levels of optimized versus non-optimized spike sequences. 293T cells were transfected by pGX9501, pVAX1-S-WT, and pVAX1 for 48hrs and lysed for RT-PCR (A) and Western blotting (B), respectively. (C) Balb/c mice were immunized by each construct at 25ug intramuscularly once and antisera samples 14 days later were used analyzed against S1 recombinant protein in ELISA.

Figure 2. Effects of Antibody Production and Functional Assay. A, The scheme of mice immunizations. B, C57BL/6, or Balb/c mice ($n \geq 5$ per group) were either immunized with pVAX1 (blue circle) or vaccinated with pVAX1-S-WT (red square) and pGX9501 (green triangle) intramuscularly, following by electroporation. Serum IgG binding titers (mean \pm SEM) to SARS-CoV-2 pre-S1, S2, and RBD were measured on day 28. C, Blocking abilities of RBD binding to the hACE2 with serum samples at serial dilutions on day 28. Data shown represent mean blocking efficiency (mean \pm SEM) for the five mice.

Figure 3. pGX9501 protects against disease challenges with SARS-CoV-2. Mice treated with the vaccine was challenged by SARS-CoV-2 (10^5 TCID₅₀) in a volume of 100 μ l 7days after the second immunization (single dose group was challenged by virus 14 days after immunization). Five days after the challenge, Serum was collected for anti-s1 ELISA(A) and Lung was harvested for measuring virus load by qRT-PCR(B). C, Mice treated with the vaccine was challenged by SARS-CoV-2 (10^5 TCID₅₀) in a volume of 100 μ l 7days after the second immunization (single dose group was challenged by virus 14 days after immunization). Serum was collected for ELISA to evaluate the Neutralizing antibody. D, The histochemistry analysis of lung after H&E staining.

Figure 4. pGX9501 promoted TH1-associated cytokine and did not affect TH2-associated cytokine. Single suspension of splenocytes and lymphoid cells of lymph nodes harvested from C57BL/6 (A) or BALB/c (B) mice immunized were stimulated with 10 mg/mL SARS-CoV-2 peptide pools in vitro for 4 to 6 hours, and IFN- \square production of CD4 $^{+}$ T cells was measured by flow cytometry. Both in C57BL/6 and Balb/C mice model. The specific Th2-cytokine expression was verified with the SARS-CoV-2 peptide pool.

Figure 5. pGX9501 derived more effective specific cytotoxic lymphocyte(CTL) killing ability in vivo and enhanced cytotoxic cytokine expression of specific CD8 $^{+}$ T cell. Single suspension lymphocytes of spleens or lymph nodes from immunized C57BL/6 (A) and Balb/C (B) mice were stimulated with 10 mg/mL SARS-CoV-2 peptide pools in vitro for 4 to 6 hours. Levels of IFN- γ and TNF- α production in CD8 $^{+}$ T cells were measured by flow cytometry. C, Antigen specific cytotoxic lymphocyte(CTL) killing ability was evaluated by an in vivo CTL assay. Target cells at 4×10^6 /ml from naïve mice labelled with a higher concentration of eFlour450 were incubated with 10 mg/mL SARS-CoV-2 peptide pools in vitro for 4-6h before transferring into the immunized mice intravenously. The intensity of eFlour450 peptide labelled target cells was compared with the non-peptide labelled negative control cells after 5 hrs by flow cytometry.

References:

- ¹ The species Severe acute respiratory syndrome-related coronavirus: classifying 2019-nCoV and naming it SARS-CoV-2. *NAT MICROBIOL* **5** 536 (2020).
- ² Poland, G. A., Tortoises, hares, and vaccines: A cautionary note for SARS-CoV-2 vaccine development. *VACCINE* **38** 4219 (2020).
- ³ Amanat, F. & Krammer, F., SARS-CoV-2 Vaccines: Status Report. *IMMUNITY* **52** 583 (2020).
- ⁴ Sakamoto, A. *et al.*, ACE2 (Angiotensin-Converting Enzyme 2) and TMPRSS2 (Transmembrane Serine Protease 2) Expression and Localization of SARS-CoV-2 Infection in the Human Heart. *Arteriosclerosis, Thrombosis, and Vascular Biology* (2020).
- ⁵ Huang, W. C. *et al.*, SARS-CoV-2 RBD Neutralizing Antibody Induction is Enhanced by Particulate Vaccination. *ADV MATER* **32** 2005637 (2020).
- ⁶ Berger, I. & Schaffitzel, C., The SARS-CoV-2 spike protein: balancing stability and infectivity. *CELL RES* **30** 1059 (2020).
- ⁷ Alarcon, J. B., Waine, G. W. & McManus, D. P., DNA vaccines: technology and application as anti-parasite and anti-microbial agents. *Adv Parasitol* **42** 343 (1999).
- ⁸ Rice, J., Ottensmeier, C. H. & Stevenson, F. K., DNA vaccines: precision tools for activating effective immunity against cancer. *NAT REV CANCER* **8** 108 (2008).
- ⁹ Robinson, H. L. & Pertmer, T. M., DNA vaccines for viral infections: basic studies and applications. *ADV VIRUS RES* **55** 1 (2000).
- ¹⁰ Tebas, P. *et al.*, Safety and Immunogenicity of an Anti-Zika Virus DNA Vaccine - Preliminary Report. *N Engl J Med* (2017).
- ¹¹ Modjarrad, K. *et al.*, Safety and immunogenicity of an anti-Middle East respiratory syndrome coronavirus DNA vaccine: a phase 1, open-label, single-arm, dose-escalation trial. *LANCET INFECT DIS* **19** 1013 (2019).
- ¹² Muthumani, K. *et al.*, A synthetic consensus anti-spike protein DNA vaccine induces protective immunity against Middle East respiratory syndrome coronavirus in nonhuman primates. *SCI TRANSL MED* **7** 132r (2015).
- ¹³ Yang, Z. Y. *et al.*, A DNA vaccine induces SARS coronavirus neutralization and protective immunity in mice. *NATURE* **428** 561 (2004).
- ¹⁴ La Gruta, N. L. & Turner, S. J., T cell mediated immunity to influenza: mechanisms of viral control. *TRENDS IMMUNOL* **35** 396 (2014).
- ¹⁵ Huang, W. C. *et al.*, SARS-CoV-2 RBD Neutralizing Antibody Induction is Enhanced by Particulate Vaccination. *ADV MATER* **32** e2005637 (2020).
- ¹⁶ Smith, T. *et al.*, Immunogenicity of a DNA vaccine candidate for COVID-19. *NAT COMMUN* **11** 2601 (2020).
- ¹⁷ Murasawa, S. *et al.*, Identification of a negative cis-regulatory element and trans-acting protein that inhibit transcription of the angiotensin II type 1a receptor gene. *J BIOL CHEM* **270** 24282 (1995).
- ¹⁸ Gupta, M., Zak, R., Libermann, T. A. & Gupta, M. P., Tissue-restricted expression of the cardiac alpha-myosin heavy chain gene is controlled by a downstream repressor element containing a palindrome of two ets-binding sites. *MOL CELL BIOL* **18** 7243 (1998).
- ¹⁹ Dispineri, S. *et al.*, Neutralizing antibody responses to SARS-CoV-2 in symptomatic COVID-19 is persistent and critical for survival. *NAT COMMUN* **12** 2670 (2021).
- ²⁰ Addetia, A. *et al.*, Neutralizing Antibodies Correlate with Protection from SARS-CoV-2 in

Humans during a Fishery Vessel Outbreak with a High Attack Rate. *J CLIN MICROBIOL* **58** (2020).

²¹ Wan, J. *et al.*, Human-IgG-Neutralizing Monoclonal Antibodies Block the SARS-CoV-2 Infection. *CELL REP* **32** 107918 (2020).

²² Jones, B. E. *et al.*, The neutralizing antibody, LY-CoV555, protects against SARS-CoV-2 infection in nonhuman primates. *SCI TRANSL MED* **13** f1906 (2021).

²³ Shi, R. *et al.*, A human neutralizing antibody targets the receptor-binding site of SARS-CoV-2. *Nature (London)* **584** 120 (2020).

²⁴ Wen, J. *et al.*, Dengue virus-reactive CD8(+) T cells mediate cross-protection against subsequent Zika virus challenge. *NAT COMMUN* **8** 1459 (2017).

²⁵ Hassert, M., Harris, M. G., Brien, J. D. & Pinto, A. K., Identification of Protective CD8 T Cell Responses in a Mouse Model of Zika Virus Infection. *FRONT IMMUNOL* **10** 1678 (2019).

²⁶ Bolland, C. M. & Heslop, H. E., T cells for viral infections after allogeneic hematopoietic stem cell transplant. *BLOOD* **127** 3331 (2016).

²⁷ Kolls, J. K., CD4(+) T-cell subsets and host defense in the lung. *IMMUNOL REV* **252** 156 (2013).

²⁸ Larena, M., Regner, M., Lee, E. & Lobigs, M., Pivotal role of antibody and subsidiary contribution of CD8+ T cells to recovery from infection in a murine model of Japanese encephalitis. *J VIROL* **85** 5446 (2011).

²⁹ Prestwood, T. R. *et al.*, Gamma interferon (IFN-gamma) receptor restricts systemic dengue virus replication and prevents paralysis in IFN-alpha/beta receptor-deficient mice. *J VIROL* **86** 12561 (2012).

³⁰ Zhao, J., Zhao, J. & Perlman, S., T cell responses are required for protection from clinical disease and for virus clearance in severe acute respiratory syndrome coronavirus-infected mice. *J VIROL* **84** 9318 (2010).

³¹ Liu, W. J. *et al.*, T-cell immunity of SARS-CoV: Implications for vaccine development against MERS-CoV. *ANTIVIR RES* **137** 82 (2017).

³² Bonifacius, A. *et al.*, COVID-19 immune signatures reveal stable antiviral T cell function despite declining humoral responses. *IMMUNITY* **54** 340 (2021).

³³ Mathew, D. *et al.*, Deep immune profiling of COVID-19 patients reveals distinct immunotypes with therapeutic implications. *SCIENCE* **369** (2020).

³⁴ Zhang, G. *et al.*, Analysis of clinical characteristics and laboratory findings of 95 cases of 2019 novel coronavirus pneumonia in Wuhan, China: a retrospective analysis. *RESP RES* **21** 74 (2020).

³⁵ Zhang, X. *et al.*, Epidemiological, clinical characteristics of cases of SARS-CoV-2 infection with abnormal imaging findings. *International journal of infectious diseases : IJID : official publication of the International Society for Infectious Diseases* **94** 81 (2020).

³⁶ Wang, F. *et al.*, Characteristics of Peripheral Lymphocyte Subset Alteration in COVID-19 Pneumonia. *The Journal of infectious diseases* **221** 1762 (2020).

³⁷ Thompson, M. G. *et al.*, Prevention and Attenuation of Covid-19 with the BNT162b2 and mRNA-1273 Vaccines. *The New England journal of medicine* (2021).

³⁸ Ewer, K. J. *et al.*, T cell and antibody responses induced by a single dose of ChAdOx1 nCoV-19 (AZD1222) vaccine in a phase 1/2 clinical trial. *NAT MED* (2020).

³⁹ Alter, G. *et al.*, Immunogenicity of Ad26.COV2.S vaccine against SARS-CoV-2 variants in humans. *Nature (London)* (2021).

TABLES

Table 1. Sequence optimization score of the optimized and wild type sequences

	CAI	GC%	Negative CIS elements	Negative repeat elements
pGX9501 Spike DNA	0.92	53.84	1	0
COVID-19 WT Spike DNA	0.88	51.43	5	0

Notes:

1.CAI (codon adaptation index) was to evaluate the optimized sequence based on CIS-regulatory elements, codon usage bias, GC rich and etc. The higher CAI value is better for the optimized sequence.

2.CIS regulatory elements was including TATA box, termination signal and protein binding sites.

Table 2. Analysis of H&E staining of lung of mice challenged with SARS-CoV-2

Groups	Infiltration of inflammatory cells in alveolar septum			Infiltration of inflammatory cells around pulmonary vessels		
	None	Slight	Medium	None	Slight	Medium
1x SSC (Ctrl)	—	—	++	—	+	—
	—	+	—	—	—	—
	—	—	++	—	+	—
	—	—	++	—	+	—
	—	+	—	—	+	—
	—	—	++	—	+	—
pGX9501 (Two dose)	—	+	—	—	—	—
	—	+	—	—	+	—
	—	+	—	—	—	—
	—	+	—	—	—	—
	—	+	—	—	+	—
	—	—	++	—	+	—
pGX9501 (one dose)	—	+	—	—	+	—
	—	+	—	—	+	—
	—	+	—	—	+	—
	—	—	++	—	+	—
	—	—	—	—	+	—
	—	—	++	—	+	—

Notes:

1, “—” refer to normal without pathology.

2, “+” refer to mild histopathological change.

3, “++” refer to mild to severe interstitial pneumonia of histopathological change.

Figure 1.

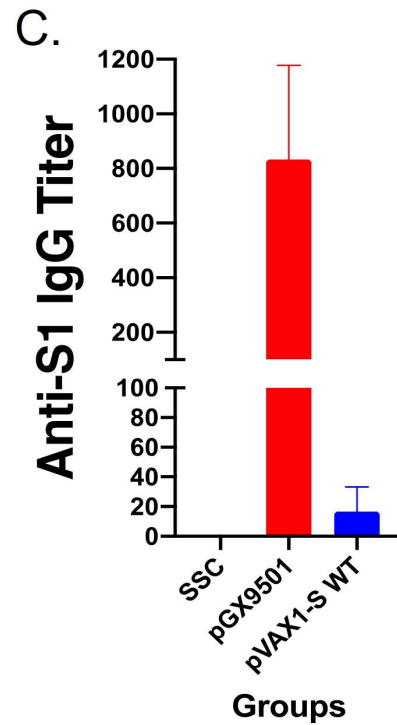
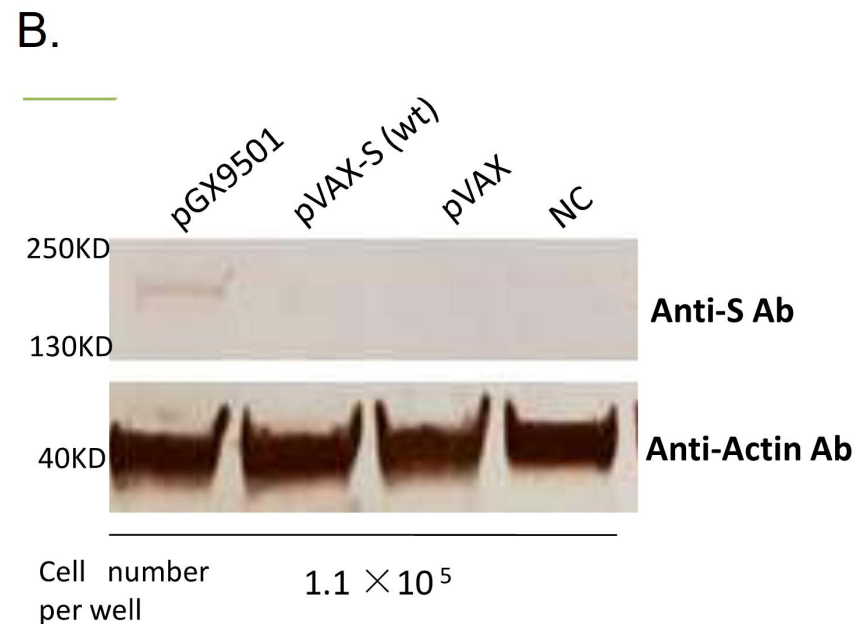
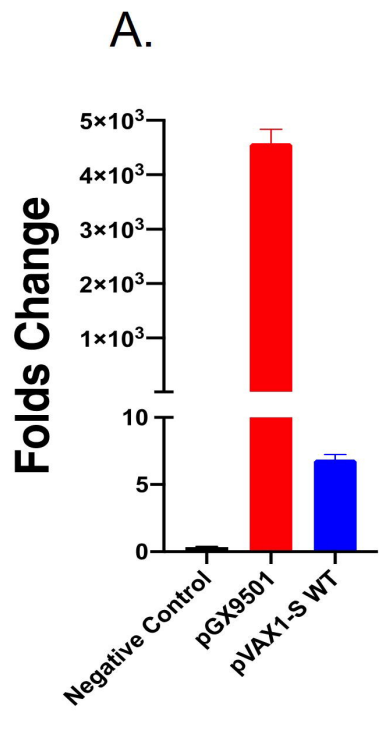


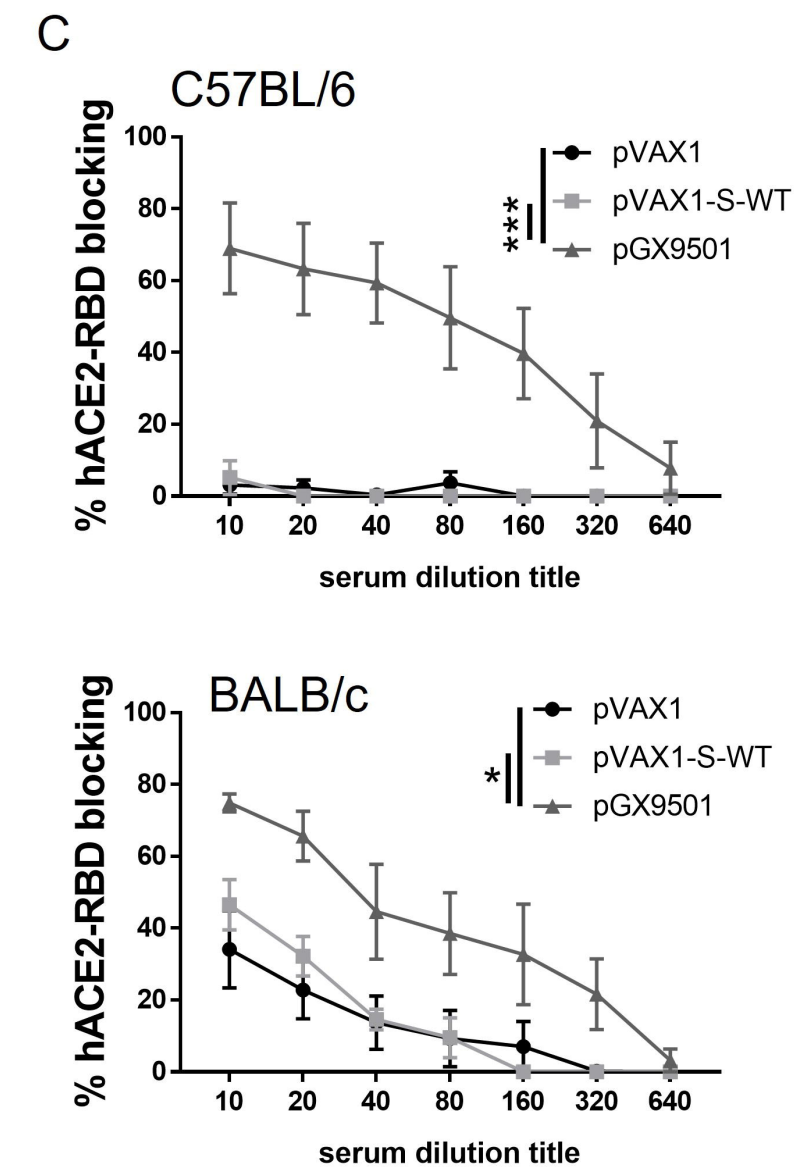
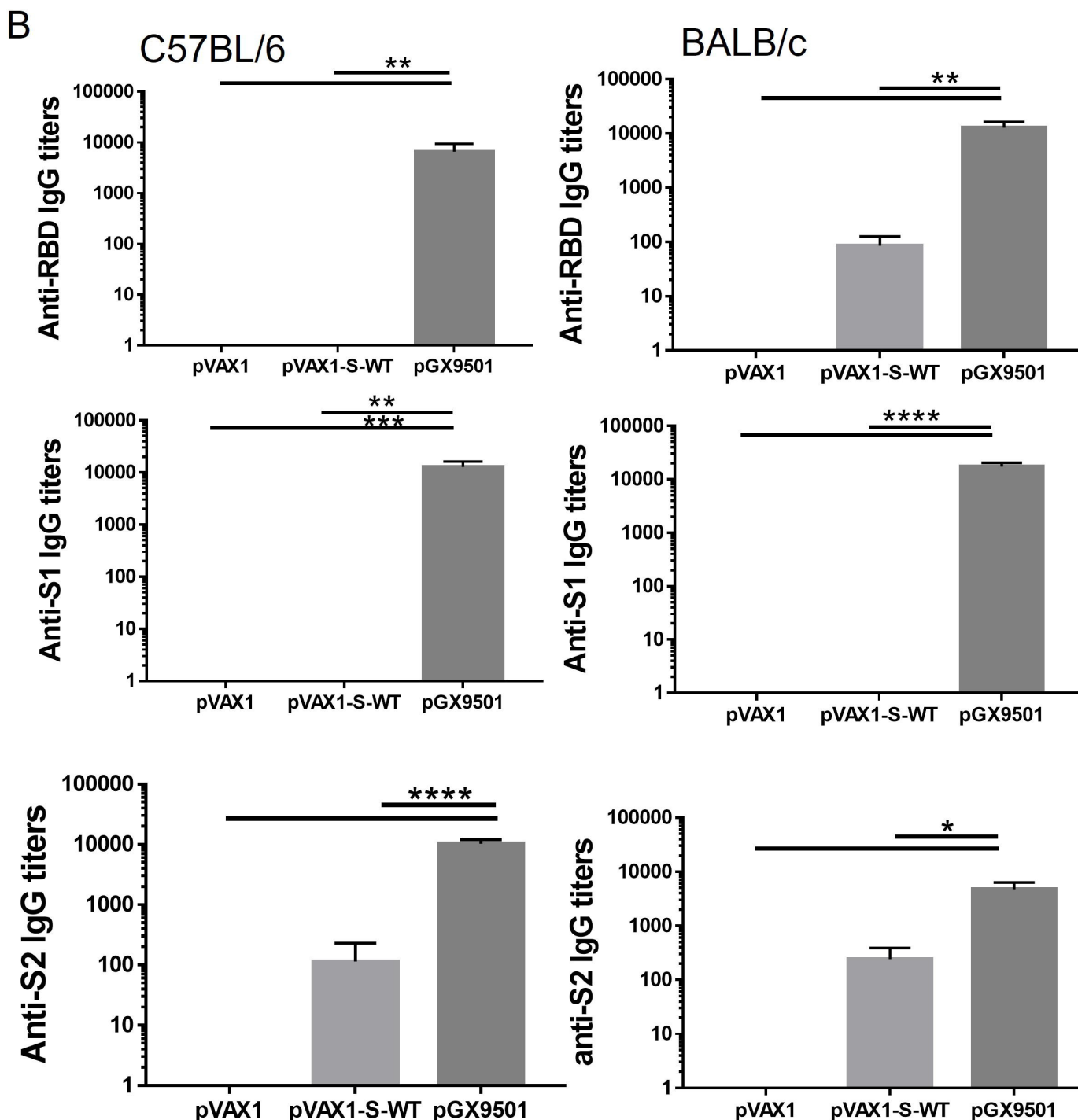
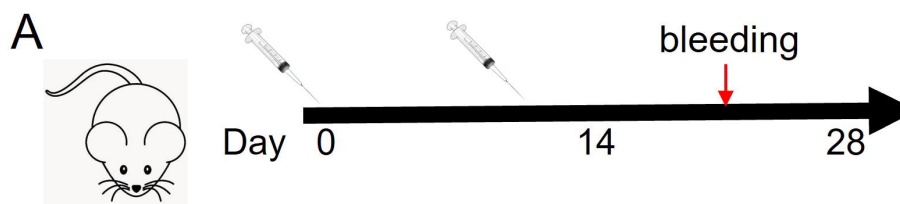
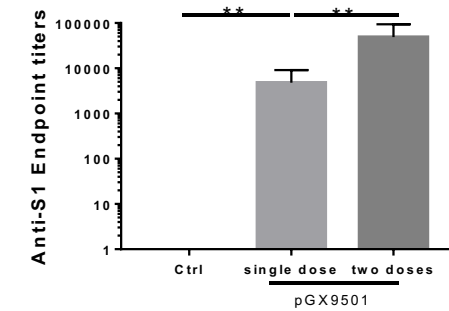
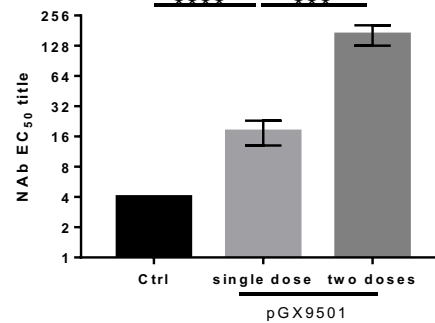
Figure 2.

Figure 3.

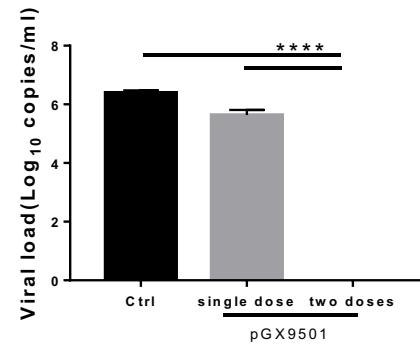
A.



B.



C.



D.

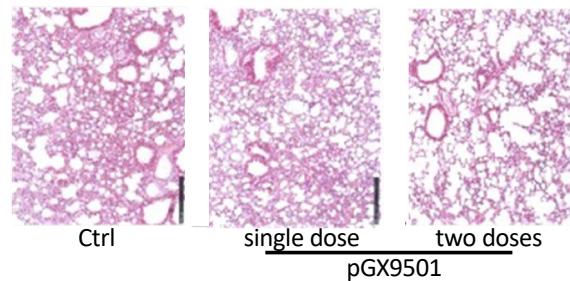
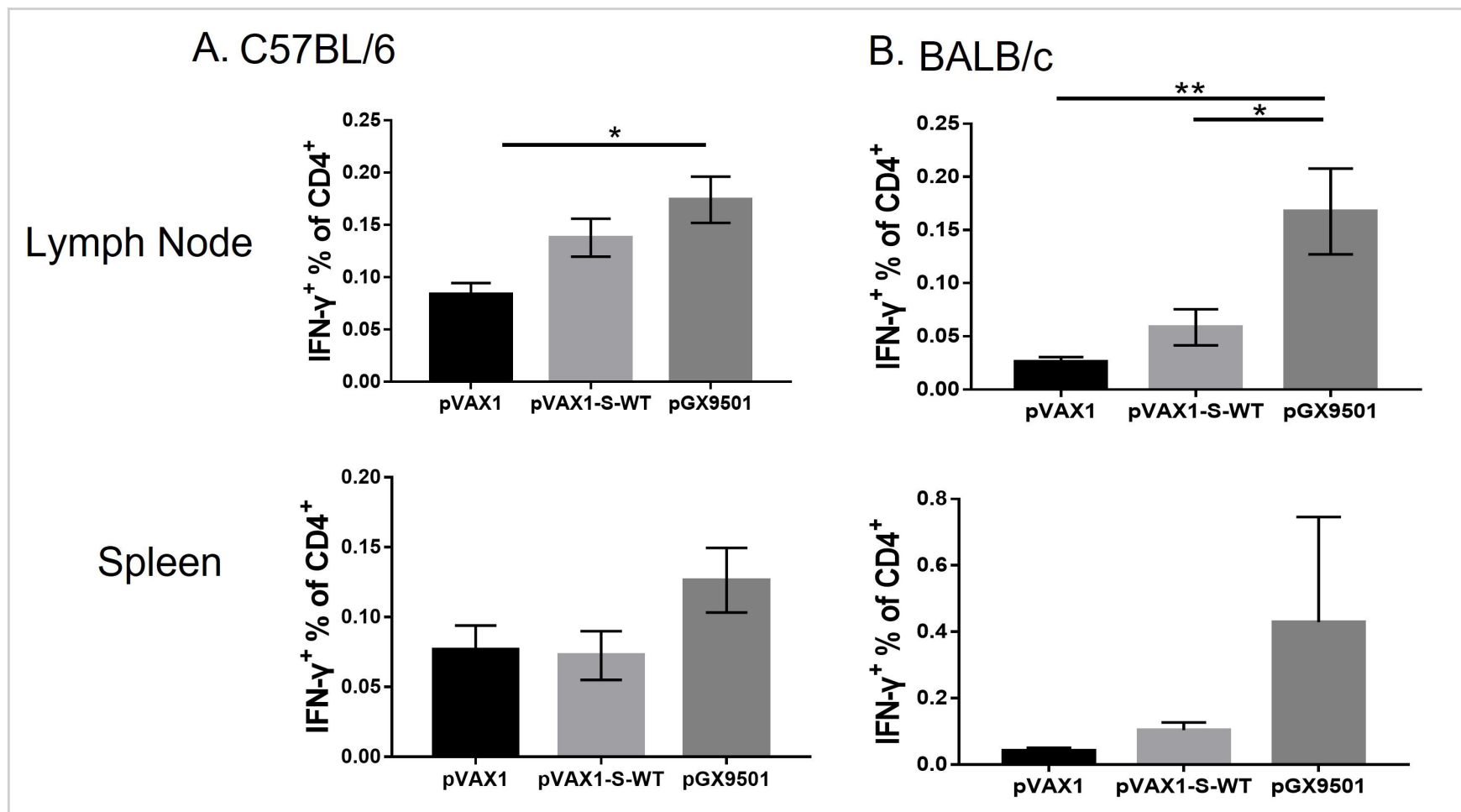
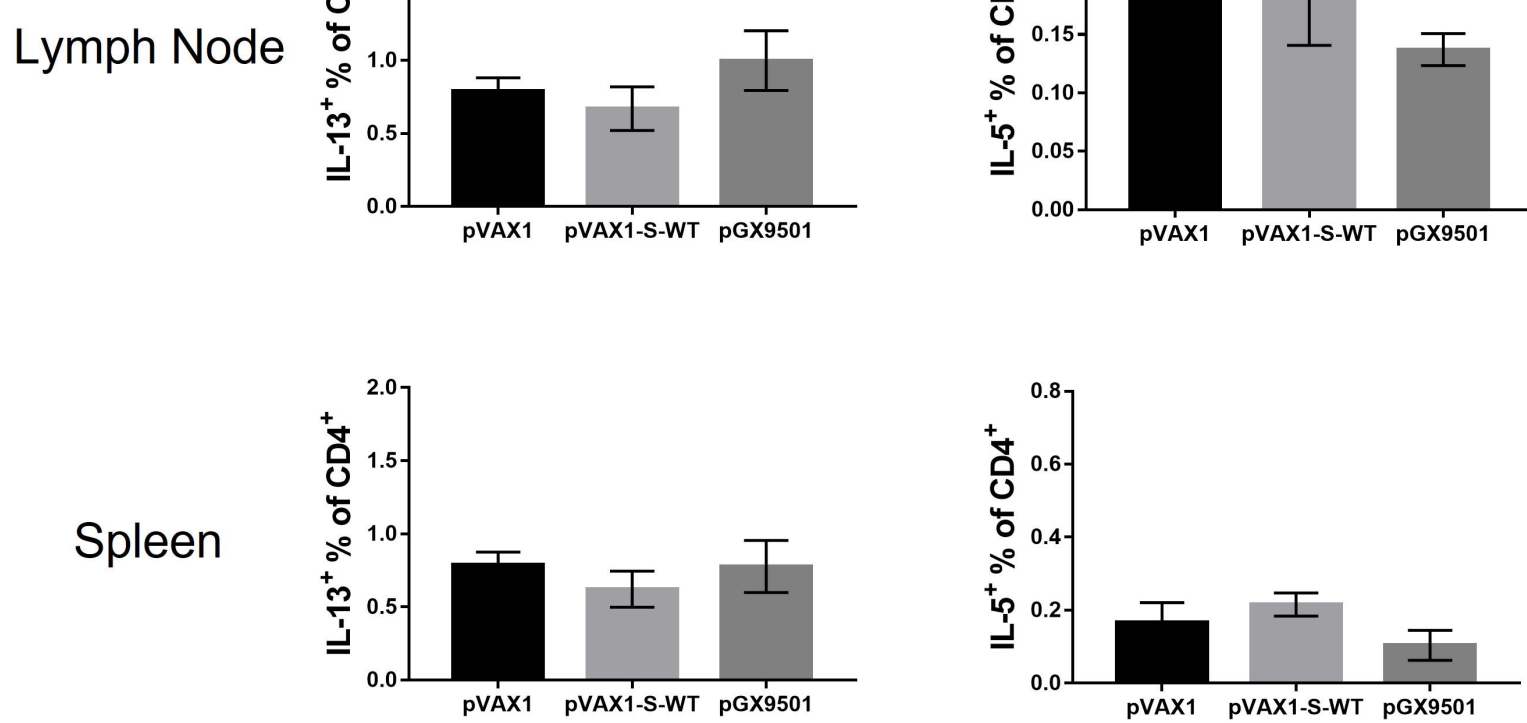


Figure 4



bioRxiv preprint doi: <https://doi.org/10.1101/2021.08.13.456164>; this version posted August 16, 2021. The copyright holder for this preprint (which was not certified by peer review) is the author/funder, who has granted bioRxiv a license to display the preprint in perpetuity. It is made available under aCC-BY 4.0 International license.

C. C57BL/6



D. BALB/c

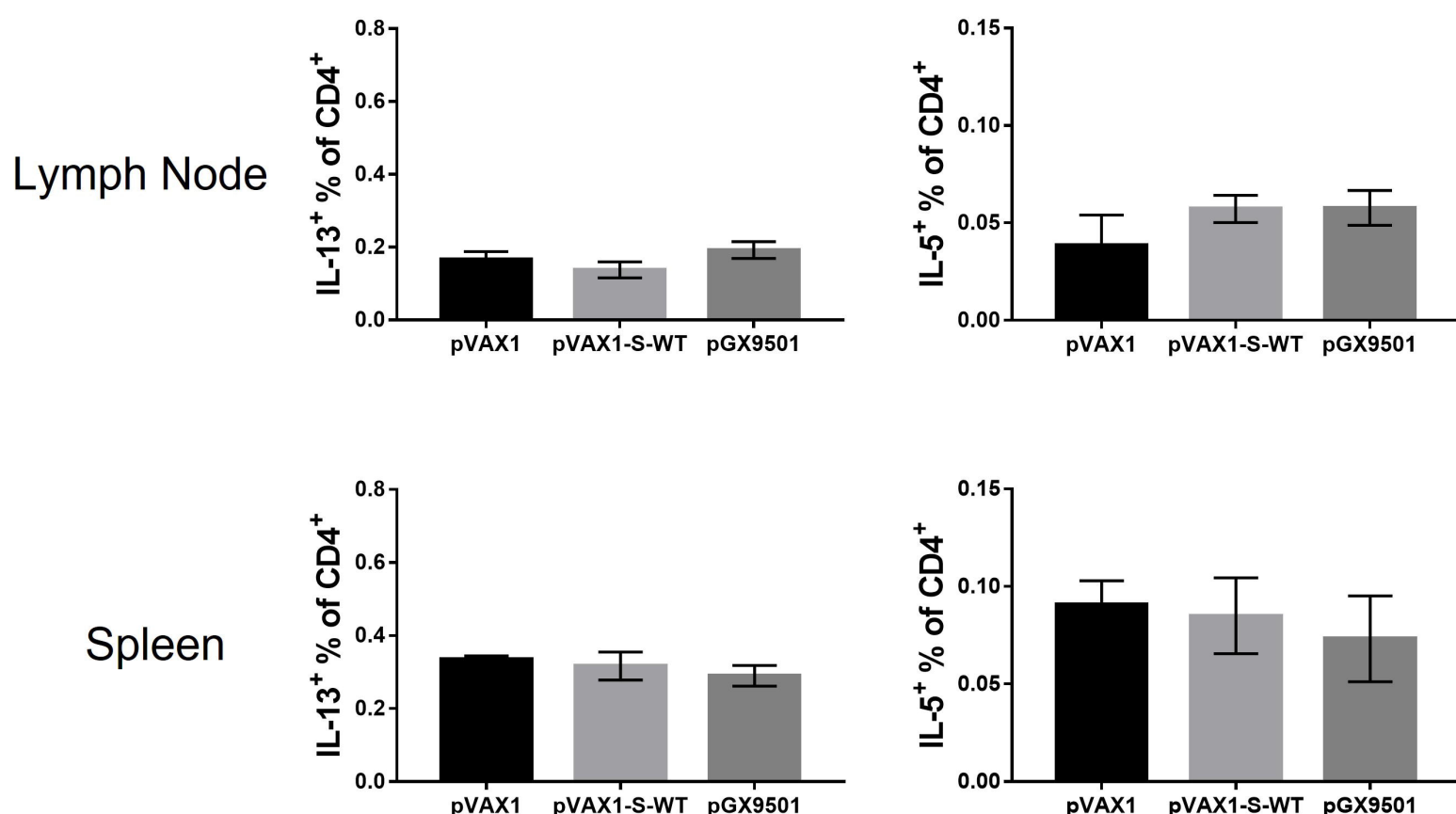


Figure 5

